($\mathbf{x} \approx 1$) between nearby individuals of the same species—will then influence the shape of the abundance distribution in larger patches in a testable manner. Nevertheless, an abundance distribution skewed toward rarity relative to the lognormal still results as long as the curvature in $z(i)$ is not extreme. Secondly, ecosystems are heterogeneous with respect to habitat quality, and thus quantities like $S(A_i)$ and $P_i(n)$ depend on which patch of area A_i is censused. Moreover, the minimum area per individual (A_m) will differ among species and among individuals in a species and thus can be defined only statistically (especially for motile organisms). Thus all statements we have made about the number of species, or the number of individuals within a particular species, in a patch of area A refer to the average over all the nonoverlapping patches of area A that comprise the system.

We have demonstrated that self-similarity theory provides an overarching framework within which empirically supported patterns in ecology are unified, new and plausible results are derived, and the connection between the SAR and the lognormal abundance distribution is questioned. Because our recursion relation for the species-abundance distribution is derived under the assumption of self-similarity, it may be more widely applicable to other spatial arrays of types of objects or to the distribution of energy fluctuations in turbulent media (*25*).

References and Notes

1. K. J. Gaston, *Rarity* (Chapman & Hall, London, 1994).
2. O. Arhennius, *J. Ecol.* **9**, 95 (1921).
3. M. L. Rosenzweig, *Species Diversity in Space and Time* (Cambridge Univ. Press, Cambridge, 1995).
4. F. W. Preston, *Ecology* **43**, 185 (1962).
5. R. M. May, in *Ecology and Evolution of Communities*, M. L. Cody and J. M. Diamond, Eds. (Belknap Press, Cambridge, MA, 1975), pp. 81–120.
6. G. Sugihara, *Am. Nat.* **116**, 770 (1980).
7. S. P. Hubbell and R. C. Foster, in *Conservation Biology: The Science of Scarcity and Diversity*, M. Soule, Ed. (Sinauer, Sunderland, MA 1986), pp. 205–231.
8. R. Condit *et al.*, *J. Ecol.* **84**, 549 (1996).
9. F. W. Preston, *Ecology* **29**, 254 (1948); S. Nee, P. H. Harvey, R. M. May, *Proc. R. Soc. London B* **243**, 161 (1991); T. M. Blackburn and K. J. Gaston, *Am. Nat.* **151**, 68 (1998).
10. B. Stone *et al.*, *British Birds* **90**, 1 (1997).
11. R. A. Kempton and L. R. Taylor, *J. Anim. Ecol.* **43**, 381(1974).
12. W. A. Leitner and M. L. Rosenzweig, *Oikos* **79**, 503 (1997).
13. B. Mandlebrot, *The Fractal Geometry of Nature* (Freeman, San Francisco, 1983).
14. Note that we are implicitly assuming symmetry as well as self-similarity, so that the fraction of the species found in A_i that are to be found in at least the left half of A_i and the fraction found in at least the right half are both equal to **a**.
15. J. Harte and A. Kinzig, *Oikos* **80**, 417 (1997).
16. An equivalent expression for the $P_i(n)$ is obtained by writing $Q_i = \Sigma_n q^n P_i(n)$ and noting that Eq. 4 implies the simpler recursion relation $Q_i = \mathbf{x}Q_{i+1} + (1 - \mathbf{x})(Q_{i+1})^2$, where $Q_m = q$. Unfortunately this relation is no more analytically tractable than is Eq. 8.
17. Analytical solutions for the first few values of n include $P_i(1) = \mathbf{x}^{m-i}$, $P_i(2) = \mathbf{x}^{m-i-1}(1 - \mathbf{x}^{m-i})$, and $P_i(3) = 2(\mathbf{x}^{m-i-1})(1 - \mathbf{x}^{m-i})(1 - \mathbf{x}^{m-i-1})/(1 + \mathbf{x})$. Note that when $n = 1$, $i \leq m$; when $n = 2$, $i \leq m - 1$; and when $n = 3$, $i \leq m - 2$. For each value of i, the maximum value of n is $n_{max} = 2^{m-i}$, and for that value the analytical expression $P_i(n_{max}) = (1 - \mathbf{x})^{(n_{max}-1)}$ also follows from Eq. 8.
18. For sufficiently small values of m and of x, the solutions to Eq. 8 exhibit pronounced superimposed oscillations to the left of the modal abundance when $P_0(n)$ is plotted against n, but for $x > 0.3$ and $m > 12$ these oscillations are indiscernible.
19. J. Harte, S. McCarthy, K. Taylor, A. Kinzig, M. Fischer, *Oikos*, in press.
20. M. L. Cody, in *Species Diversity in Ecological Communities*, R. Ricklefs and D. Schluter, Eds. (Univ. of Chicago Press, Chicago, 1993), pp. 147–158.
21. W. E. Kunin, *Biol. Cons.* **82**, 369 (1997).
22. W. E. Kunin, *Science* **281**, 1513 (1998).
23. It can be shown from self-similarity (J. Harte and T. Blackburn, *Am. Nat.*, in press) that a plot of ln(total number of windows of area A occupied by each species) versus ln(abundance of species) yields a straight line result with slope equal to $[\ln(A_0/A)/\ln(N_0)]$, where A is the area of the censusing window, A_0 is the total area censused, and N_0 is the total abundance of all the species plotted within the broader taxonomic category. It also follows that Kunin's ln-ln curves of range versus area of census window have straight line slopes of $1 - [\ln(n_\alpha)/\ln(N_0)]$, where n_α is the abundance of the particular species.
24. I. Hanski, *Oikos* **38**, 210 (1982); I. Hanski, J. Kouki, A. Halkka, in *Historical and Geographical Determinants of Community Diversity*, R. Ricklefs and D. Schluter, Eds. (Univ. of Chicago Press, Chicago, 1993)
25. For turbulent media, it has been shown that a lognormal distribution of energy fluctuations is incompatible with self-similarity [B. Mandelbrot, in *Lecture Notes in Physics 12: Statistical Models and Turbulence*, J. Ehlers K. Munchen, H. Weidenmuller, Eds. (Springer-Verlag, Berlin, 1971), pp. 333–351]. The self-similar distribution in Fig. 3, on the other hand, bears a striking resemblance to empirical distributions of self-similar phenomena [S. T. Bramwell, P. C. W. Holdsworth, J.-F. Pinton, *Nature* **396**, 552 (1998)].

26. Support from the Mellon Foundation and the Class of 1935 Endowed Chair at the University of California, Berkeley, was instrumental in pursuing this work. We thank H. Horn for suggesting the use of golden rectangles; D. Gay for useful discussions about recursion relations; T. Blackburn for numerous helpful conversations and insight into abundance and distribution patterns; and D. Yu, W. Watt, C. Boggs, M. Fischer, W. Kunin, S. Pacala, and S. Saleska for useful comments on the manuscript.

16 October 1998; accepted 2 February 1999

NMDA Receptor–Mediated K^+ Efflux and Neuronal Apoptosis

S. P. Yu,* C.-H. Yeh,* U. Strasser, M. Tian, D. W. Choi†

Neuronal death induced by activating *N*-methyl-D-aspartate (NMDA) receptors has been linked to Ca^{2+} and Na^+ influx through associated channels. Whole-cell recording from cultured mouse cortical neurons revealed a NMDA-evoked outward current, I_{NMDA-K}, carried by K^+ efflux at membrane potentials positive to −86 millivolts. Cortical neurons exposed to NMDA in medium containing reduced Na^+ and Ca^{2+} (as found in ischemic brain tissue) lost substantial intracellular K^+ and underwent apoptosis. Both K^+ loss and apoptosis were attenuated by increasing extracellular K^+, even when voltage-gated Ca^{2+} channels were blocked. Thus NMDA receptor–mediated K^+ efflux may contribute to neuronal apoptosis after brain ischemia.

N-methyl-D-aspartate (NMDA) receptor–gated channels are permeable to Ca^{2+}, Na^+, and K^+ (*1*). NMDA receptor–mediated Na^+ and Ca^{2+} influx participates in synaptic transmission (*2*, *3*) and excitotoxicity (*4*). In contrast, NMDA receptor–mediated K^+ efflux has received little scrutiny, and its functional significance in either normal or abnormal states has not been defined. Stimulating NMDA receptors can induce central neuronal apoptosis (*5*, *6*), and loss of cellular K^+ may be a key step in caspase activation (*7*) and programmed cell death (*8*, *9*). We set out to test the hypothesis that NMDA receptor–mediated K^+ efflux might promote neuronal apoptosis.

To detect K^+ efflux through NMDA receptor channels, the membrane current triggered by NMDA was recorded in mouse cortical neurons by means of patch clamp whole-cell recording in an extracellular solution where Ca^{2+} and Na^+ were replaced by the impermeable cation *N*-methyl-D-glutamine (NMG) (*10*). At the membrane potential of −60 mV, where NMDA normally evokes inward currents in bathing solutions containing physiological concentrations of Na^+ and Ca^{2+}, application of 200 μM NMDA plus 10 μM glycine induced an outward current, designated here as I_{NMDA-K}, of 33 ± 6 pA (mean ± SEM, $n = 11$ cells; Fig. 1). This outward current was enlarged at depolarized membrane potentials, reaching 315 ± 39 pA at 0 mV ($n = 11$). The current-voltage curve of I_{NMDA-K} showed slight outward rectification, and the current reversed at −86 ± 4 mV ($n = 8$), near the calculated K^+ equilibrium potential of −93 mV. The I_{NMDA-K} reversal potential shifted toward more positive potentials when external K^+ was increased from 3 mM to 25 mM (Fig. 1) or when internal K^+ was decreased from 120

Center for the Study of Nervous System Injury and Department of Neurology, Washington University School of Medicine, St. Louis, MO 63110, USA.

*These authors contributed equally to this work.
†To whom correspondence should be addressed. E-mail: choid@neuro.wustl.edu

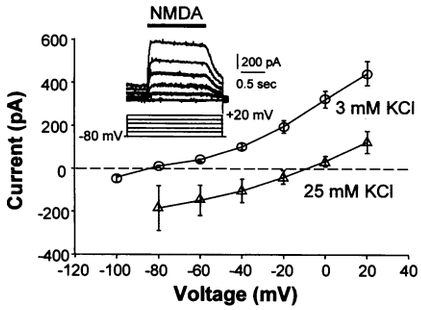

Fig. 1. NMDA receptor channel–mediated outward current I_{NMDA-K}. Local application of 200 μM NMDA plus 10 μM glycine triggered outward whole-cell currents in a Na^+/Ca^{2+}-free medium (**inset**) (*10*). Raising external K^+ from 3 mM (n = 11 cells) to 25 mM (n = 8) shifted the reversal potential of the current to the right, which is consistent with K^+ as the charge carrier. Error bars indicate mean ± SEM.

mM to 12 mM [an inward current of –29 ± 10 pA was then triggered by NMDA at –60 mV (n = 4)].

We next examined whether NMDA receptor–mediated K^+ efflux could affect neuron viability in mixed cortical cultures containing neurons and glia (12 to 13 days in vitro) (*11*, *12*). In medium containing physiological concentrations of Na^+ and Ca^{2+}, overstimulation of NMDA receptors in our cortical cultures triggered neuronal necrosis characterized by prominent, acute, cell body swelling, little or no DNA laddering, and insensitivity to protein synthesis inhibition (*4*, *13*). However, if NMDA-induced inward cation influx was attenuated by lowering extracellular Na^+ and Ca^{2+} to 30 mM and 0.1 mM, respectively (a maneuver that in itself was not toxic), adding 100 μM NMDA plus 10 μM glycine for 1 hour (followed by returning to control medium plus 10 μM MK-801) produced widespread neuronal apoptosis over the next 23 hours. This NMDA-induced apoptosis was characterized by cell body shrinkage, nuclear condensation, internucleosomal DNA fragmentation, and sensitivity to protein synthesis inhibition with cycloheximide (CHX) or caspase inhibition with Z-Val-Ala-Asp-fluoromethylketone (Z-VAD) (Fig. 2, A and B, and Fig. 3A). Neuronal cell body shrinkage preceded neuronal death (Fig 2C); neuronal cell cross-sectional area decreased from 223.0 ± 4.3 μm^2 to 146.9 ± 3.4 μm^2 at the end of the 1-hour NMDA exposure (a 34% reduction, different at $P < 0.01$; n = 206 cells per group) and was accompanied by substantial loss of intracellular K^+ (Fig. 2D) (*12*). Consistent with the hypothesis that the observed cellular K^+ loss and neuronal apoptosis were mediated by I_{NMDA-K}, they were blocked by the NMDA antagonist, 1 μM MK-801 (Fig. 3A) (cellular K^+ content was 111 ± 7% of the control at the end of the 1-hour NMDA exposure, n = 3 assays). Increasing external K^+ from 5 to 25 mM, which reduced K^+ efflux, attenuated the NMDA-induced neuronal death. High-K^+ medium may increase intracellular Ca^{2+} because of the opening of voltage-gated Ca^{2+} channels upon membrane depolarization; however, the neuroprotection by 25 mM K^+ was not affected when voltage-gated Ca^{2+} channels were blocked by addition of 5 or 10 μM gadolinium [Gd^{3+} (Fig. 3A)] (*9*). Increasing extracellular K^+ also blocked cellular K^+ loss (K^+ content at the end of the NMDA treatment was 105 ± 4% of the control, n = 3) and attenuated cell body shrinkage (the cell cross-sectional areas at the end of the NMDA exposure were 66 ± 2% and 80 ± 3% of controls in 5 and 25 mM K^+ medium, respectively; $P < 0.01$, $n \geq 140$ cells for each group). No additive protection was observed with the co-application of Z-VAD and 25 mM K^+ (Fig. 3A).

In cultured rat hippocampal slices, lowering extracellular Na^+ to 3.6 mM for 30 min induced a 20- to 40-fold increase in extracellular glutamate (*14*), probably because of a block or reversal of the Na^+-dependent high-affinity glutamate transporter on neurons and astrocytes (*15*). We used this protocol to determine whether endogenous glutamate release could induce NMDA receptor–mediated K^+ efflux and consequent neuronal apoptosis. Mixed cultures exposed for 2 hours to a medium containing 3 mM Na^+ and 0.1 mM Ca^{2+} induced shrinkage of neuronal cell bodies, followed by widespread neuronal apoptosis 22 hours later (Fig. 3B), as evidenced by morphology under electron microscopic examination and the presence of DNA laddering on agarose gel. The cell body shrinkage and cell death were attenuated by addition of one of several different NMDA antagonists or by the raising of external K^+ to 25 mM,

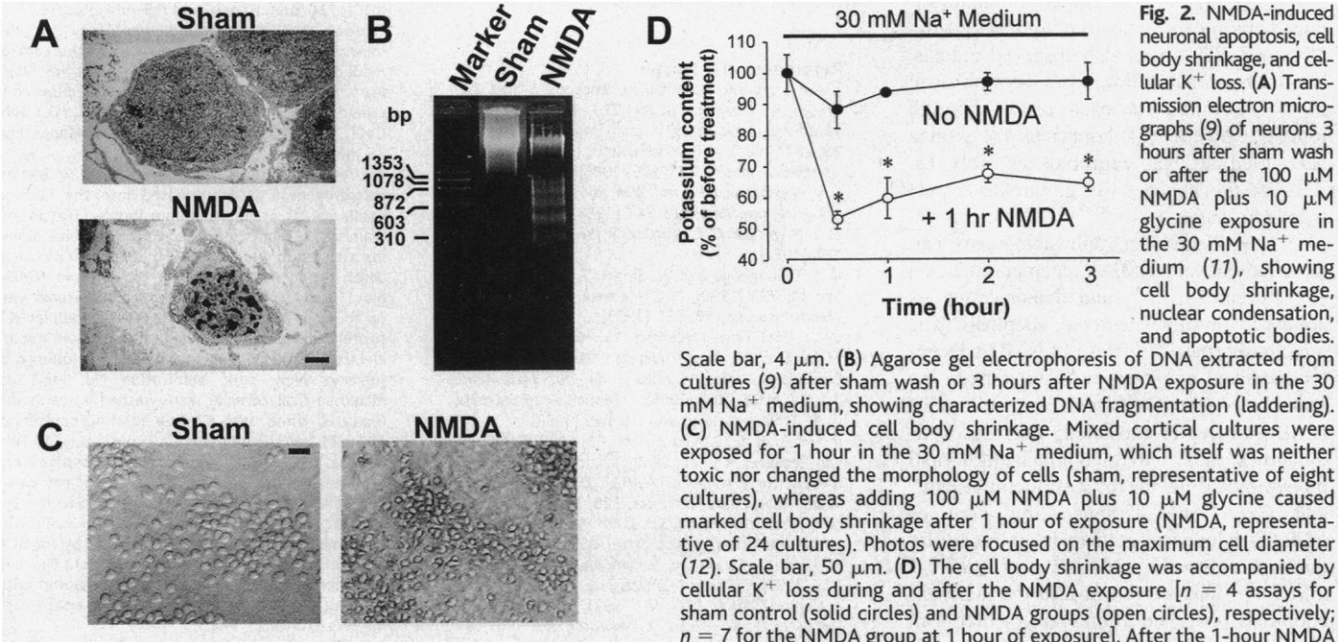

Fig. 2. NMDA-induced neuronal apoptosis, cell body shrinkage, and cellular K^+ loss. (**A**) Transmission electron micrographs (*9*) of neurons 3 hours after sham wash or after the 100 μM NMDA plus 10 μM glycine exposure in the 30 mM Na^+ medium (*11*), showing cell body shrinkage, nuclear condensation, and apoptotic bodies. Scale bar, 4 μm. (**B**) Agarose gel electrophoresis of DNA extracted from cultures (*9*) after sham wash or 3 hours after NMDA exposure in the 30 mM Na^+ medium, showing characterized DNA fragmentation (laddering). (**C**) NMDA-induced cell body shrinkage. Mixed cortical cultures were exposed for 1 hour in the 30 mM Na^+ medium, which itself was neither toxic nor changed the morphology of cells (sham, representative of eight cultures), whereas adding 100 μM NMDA plus 10 μM glycine caused marked cell body shrinkage after 1 hour of exposure (NMDA, representative of 24 cultures). Photos were focused on the maximum cell diameter (*12*). Scale bar, 50 μm. (**D**) The cell body shrinkage was accompanied by cellular K^+ loss during and after the NMDA exposure [n = 4 assays for sham control (solid circles) and NMDA groups (open circles), respectively; n = 7 for the NMDA group at 1 hour of exposure]. After the 1-hour NMDA exposure, cells were returned to control medium containing 10 μM MK-801. No cell death was found at this time (n = 8 cultures) by either propidium iodide staining or LDH release (*12*), although 3 hours later, about 30% cell death was detected. Co-applied MK-801 (1 μM) or raising the extracellular K^+ concentration to 25 mM prevented the K^+ loss. Asterisks indicate difference from controls at each time point or before treatment [$P < 0.01$, one-way analysis of variance (ANOVA)].

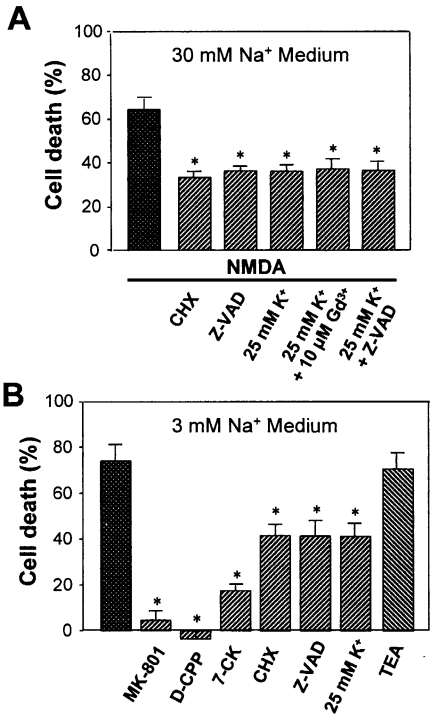

Fig. 3. NMDA- and endogenous glutamate–induced neuronal apoptosis. (**A**) Neuronal apoptosis triggered by exogenously added NMDA. Mixed cortical cultures were exposed for 1 hour to 100 μM NMDA in the low-Na^+ (30 mM), low-Ca^{2+} (0.1 mM) medium and then returned to control medium containing 10 μM MK-801. Cell death was assayed by LDH release and cell counts 24 hours after the onset of insult (*12*). Exposure to the 30 mM Na^+ solution alone for 1 hour caused no perceptible cell death. NMDA-triggered neuronal death was attenuated by co-applied CHX (1 μg/ml) or 100 μM Z-VAD or by raising extracellular K^+ to 25 mM. The 25 mM K^+ effect was not affected by adding the Ca^{2+} channel antagonist Gd^{3+} (5 or 10 μM); Gd^{3+} alone at these concentrations had no effect on NMDA-induced apoptosis [n = 4 cultures (*23*)]. No synergy was seen when both Z-VAD and 25 mM K^+ were applied. Similar neuronal apoptotic death was induced when extracellular Mg^{2+} was reduced from 2 to 1 mM (n = 12 cultures), a concentration that precluded a NMDA receptor–mediated, Mg^{2+} influx–induced neuronal necrosis (*24*). The CHX- and Z-VAD–insensitive residual cell death was likely due to necrosis. (**B**) Neuronal apoptosis triggered by endogenous glutamate. Exposure for 2 hours to the bathing medium containing 3 mM Na^+ and 0.1 mM Ca^{2+}, followed by return to normal medium plus MK-801 (10 μM) and 6-cyano-7-nitroquinoxaline-2,3-dione (100 μM), triggered substantial neuronal cell death 22 hours later (leftmost bar) (*11*). This death was largely blocked if the NMDA antagonists MK-801 (1 μM) or D-3-(2-carboxypiperazin-4-yl-)-propyl-1-phosphonic acid (D-CPP) (100 μM) or the glycine antagonist 7-chlorokynurenate (7-CK) (100 μM) was included during the 2-hour exposure. CHX (1 μg/ml), 100 μM Z-VAD, or 25 mM K^+, but not TEA (5 mM), also attenuated neuronal death. The Ca^{2+} channel antagonist Gd^{3+} (5 or 10 μM) did not occlude the protective effect by 25 mM K^+. Twelve cultures were used for each test in (A) and (B). Asterisks indicate difference from the 3 mM Na^+ medium alone ($P < 0.01$, one-way ANOVA).

but not by addition of the K^+ channel blocker tetraethylammonium (TEA) (5 mM) (Fig. 3B). Endogenous glutamate-induced apoptosis, sensitive to CHX, MK-801, or Z-VAD, was also observed in nearly pure neuronal cultures (12 days in vitro; n = 8 cultures for each test), although longer exposure (24 hours) to the 3 mM Na^+ medium was required, possibly reflecting the absence of glutamate export from glial cells.

We have thus electrophysiologically isolated the outward NMDA receptor–mediated K^+ current $I_{NMDA\text{-}K}$ and demonstrated its ability to promote neuronal apoptosis. The ionic basis (the K^+ efflux) of NMDA receptor–mediated apoptosis is distinct from the ionic basis (the Ca^{2+} and Na^+ influx) of NMDA receptor–mediated necrosis. Although the latter may predominate at normal physiological levels of extracellular Na^+ and Ca^{2+}, the demonstration here of NMDA-induced apoptosis in extracellular medium containing 30 mM Na^+ and 0.1 mM Ca^{2+} may be relevant to the neuronal apoptosis observed after brain ischemia in vivo (*16*), where comparable concentrations of these ions have been measured (*17*). NMDA receptor–mediated K^+ efflux may also contribute to neuronal apoptosis under other conditions, as it occurs even in the presence of normal concentrations of extracellular Ca^{2+} and Na^+ (*1*).

References and Notes

1. J. A. Harvey and H. McIlwain, *Biochem. J.* **108**, 269 (1968); R. Anwyl, *J. Physiol.* **273**, 367 (1977); V. I. Taichberg, O. Goldberg, A. Luini, *Mol. Cell. Biochem.* **39**, 281 (1981); A. B. MacDermott, M. L. Mayer, G. L. Westbrook, *Nature* **321**, 519 (1986); M. L. Mayer and G. L. Westbrook, *J. Physiol.* **394**, 501 (1987); P. Ascher and L. Nowak, *ibid.* **399**, 247 (1988).
2. M. L. Mayer and G. L. Westbrook, *Prog. Neurobiol.* **28**, 197 (1987).
3. G. L. Collingridge and W. Singer, *Trends Pharmacol. Sci.* **11**, 290 (1990); R. C. Malenka and R. A. Nicoll, *Trends Neurosci.* **16**, 521 (1993).
4. D. W. Choi, *Trends Neurosci.* **11**, 465 (1988).
5. M. Ankarcrona *et al.*, *Neuron* **15**, 961 (1995); E. Bonfoco, D. Krainc, M. Ankarcrona, *Proc. Natl. Acad. Sci. U.S.A.* **92**, 7162 (1995); L. Tenneti, D. M. D'Emilia, C. M. Troy, *J. Neurochem.* **71**, 946 (1998).
6. F. Finiels *et al.*, *J. Neurochem.* **65**, 1027 (1995); M. van Lookeren Campagne, P. J. Lucassen, J. P. Vermeulen, *Eur. J. Neurosci.* **7**, 1627 (1995); Z. H. Qin, Y. Wang, T. N. Chase, *Brain Res.* **725**, 166 (1996); Y. Du *et al.*, *Proc. Natl. Acad. Sci. U.S.A.* **94**, 11657 (1997); H. Kawasaki *et al.*, *J. Biol. Chem.* **272**, 18518 (1997); M. Lesort, F. Esclaire, C. Yardin, *Neurosci. Lett.* **221**, 213 (1997); C. Portera-Cailliau, D. L. Price, L. J. Martin, *J. Comp. Neurol.* **378**, 88 (1997); F. Ogden, M. A. DeCoster, F. G. Bazan, *J. Neurosci. Res.* **53**, 677 (1998).
7. D. Perregaux and C. A. Gabel, *J. Biol. Chem.* **269**, 15195 (1994); I. Walev, K. Reske, M. Palmer, A. Valeva, S. Bhakdi, *EMBO J.* **14**, 1607 (1995); C. D. Bortner, F. M. Hughes Jr., J. A. Cidlowski, *J. Biol. Chem.* **272**, 32436 (1997); F. M. Hughes Jr., C. D. Bortner, G. D. Purdy, J. A. Cidlowski, *ibid.*, p. 30567.
8. S. P. Yu *et al.*, *Soc. Neurosci. Abstr.* **22**, 1721 (1996); S. P. Yu, Z. S. Farhangrazi, H. S. Ying, C.-H. Yeh, D. W. Choi, *Neurobiol. Dis.* **5**, 81 (1998); Y. Inai *et al.*, *Cell Struct. Funct.* **22**, 555 (1997); J. V. McCarthy and T. G. Cotter, *Cell Death Differ.* **4**, 756 (1997); A. J. Bilney and A. W. Murray, *FEBS Lett.* **424**, 221 (1998); B. Dallaporta *et al.*, *J. Immunol.* **160**, 5605 (1998).
9. S. P. Yu *et al.*, *Science* **278**, 114 (1997).
10. Whole-cell recording was performed in 35-mm dishes of cortical neurons cultured for 10 to 13 days in vitro, as described previously (*9*, *18*, *19*). Neurons 15 to 20 μm in diameter were voltage-clamped with an EPC-7 amplifier (List-Electronic, Germany) using electrodes with tip resistance of 8 to 12 megohms (fire-polished). NMDA and glycine were locally applied by means of the DAD-12 perfusion system (Adams and List, New York). Current and voltage traces were displayed and stored on a Macintosh computer (Quadra 950, Apple Computer) using the software PULSE (HEKA Electronik, Germany). The external solution contained 120 mM NMG, 3 or 25 mM KCl, 1 mM $MgCl_2$, 10 mM Hepes, 10 mM glucose, and 0.5 μM tetrodotoxin. The internal solution contained 120 mM KCl, 2 mM Na_2–adenosine triphosphate, 10 mM Hepes, and 5 mM BAPTA. The solution pH was 7.3, and recordings were made at room temperature.
11. Primary cortical cultures were used (*9*, *19*, *20*). Dissociated embryonic neocortices from mice at 15 to 17 days of gestation were plated onto a preestablished glial monolayer at a density of 3.5 hemispheres per 10 ml in 35-mm culture dishes (for patch clamp) or in 24-well plates (for toxicity) in Eagle's minimal essential medium (MEM, Earle's salts; Gibco-BRL, Gaithersburg, MD) supplemented with 20 mM glucose, 5% fetal bovine serum, and 5% horse serum, Medium changes were carried out as described (*19*). Nearly pure neuronal cultures were plated onto 24-well plates coated with poly-D-lysine and laminin at 4.0 hemispheres per 10 ml; nonneuronal cell growth was inhibited by cytosine arabinoside (3.3 μM) 3 days later. Cultures were kept in a 37°C humidified incubator in a 5% CO_2 atmosphere. The 30 mM Na^+ medium used in toxicity experiments contained 90 mM NMG, 30 mM $NaHCO_3$, 0.1 mM $CaCl_2$, 5 mM KCl, 2 mM $MgCl_2$, 20 mM Hepes, and 15 mM glucose. This solution had a measured osmolarity of 307 mosmol/liter, which is comparable to the control medium containing 145 mM Na^+ but no NMG (294 mosmol/liter). The 3 mM Na^+ medium contained 117 mM NMG, 3 mM $NaHCO_3$, 0.1 mM $CaCl_2$, 5 mM KCl, 2 mM $MgCl_2$, 20 mM Hepes, and 15 mM glucose.
12. Neuronal cell death was determined by lactate dehydrogenase (LDH) released into the bathing medium (*21*) or by propidium iodide (10 μM/ml) staining (*22*) and confirmed by trypan blue staining. Cell death was scaled to the near-full neuronal death produced by exposure to 300 μM NMDA plus 10 μM glycine for 24 hours in cultures prepared from the same plating. Total cellular K^+ content was examined by the K^+ selective microelectrode (Clinical Diagnostic Systems, Johnson & Johnson, New York, publication No. MP2-12). Mixed cortical cultures were washed twice at the indicated times with K^+-free solution containing 120 mM NaCl, 2 mM $MgCl_2$, 2 mM $CaCl_2$, 10 mM glucose, and 10 mM Hepes; cell membranes were disrupted by 0.1% Triton X-100 (25 μl per well); and solutions from four wells were collected for each K^+ measurement. Cell density in wells was confirmed by protein content measured by the BCA protein assay kit (Pierce, Rockford, IL). The cell maximum cross-section area was measured with the MetaMorph Imaging System (Universal Imaging, West Chester, PA).
13. C. A. Csernansky, L. M. Canzoniero, S. L. Sensi, *J. Neurosci. Res.* **38**, 101 (1994); B. J. Gwag *et al.*, *Neuroscience* **77**, 393 (1997).
14. M. Takahashi and M. Hashimoto, *Brain Res.* **735**, 1 (1996).

15. A. Schousboe, G. Svenneby, L. Hertz, *J. Neurochem.* **29**, 999 (1977); W. B. Stallcup, K. Bulloch, E. E. Baetge, *ibid.* **32**, 57 (1979); D. Nicholls and D. Attwell, *Trends Pharmacol. Sci.* **11**, 462 (1990); M. Szatkowski, B. Barbour, D. Attwell, *Nature* **348**, 443 (1990).
16. M. D. Linnik, R. H. Zobrist, M. D. Hatfield, *Stroke* **24**, 2002 (1993); Y. Li, M. Chopp, N. Jiang, *ibid.* **26**, 1252 (1995); D. W. Choi, *Curr. Opin. Neurobiol.* **6**, 667 (1996); C. Du, R. Hu, C. A. Csernansky, *J. Cereb. Blood Flow Metab.* **16**, 195 (1996); J. Chen *et al.*, *J. Neurochem.* **69**, 232 (1997).
17. A. J. Hansen and T. Zeuthen, *Acta Physiol. Scand.* **113**, 437 (1981); A. J. Hansen, *Physiol. Rev.* **65**, 101 (1985); B. K. Siesjö, *J. Neurosurg.* **77**, 169 (1992); Y. Xie, K. Dengler, E. Zacharias, *Brain Res.* **652**, 216 (1994); T. Kristian and B. K. Siesjö, *Stroke* **29**, 705 (1998).
18. O. P. Hamill, A. Marty, E. Neher, *Pflugers Arch.* **391**, 85 (1981).
19. S. P. Yu, S. L. Sensi, L. M. T. Canzoniero, A. Buisson, D. W. Choi, *J. Physiol.* **499**, 721 (1997).
20. K. Rose, M. P. Goldberg, D. W. Choi, in *Methods in Toxicology: In Vitro Biological Systems*, C. A. Tyson and J. M. Frazier, Eds. (Academic Press, San Diego, CA, 1993), pp. 46–60.
21. J.-Y. Koh and D. W. Choi, *J. Neurosci. Methods* **20**, 83 (1987).
22. J. G. Rudolph, J. J. Lemasters, F. T. Crews, *Neurosci. Lett.* **221**, 149 (1997).
23. S. P. Yu, C. H. Yeh, U. Strasser, M. Tian, D. W. Choin, data not shown.
24. K. A. Hartnett *et al.*, *J. Neurochem.* **68**, 1836 (1997).
25. This work was supported by NIH grants NS 30337 (D.W.C.) and NS 32636 (D.W.D. and S.P.Y).

3 December 1998; accepted 9 March 1999

Ca^{2+}-Induced Apoptosis Through Calcineurin Dephosphorylation of BAD

Hong-Gang Wang,[1,2]* Nuzhat Pathan,[1]* Iryna M. Ethell,[1] Stanislaw Krajewski,[1] Yu Yamaguchi,[1] Futoshi Shibasaki,[3] Frank McKeon,[3] Tanya Bobo,[4] Thomas F. Franke,[4] John C. Reed[1]†

The Ca^{2+}-activated protein phosphatase calcineurin induces apoptosis, but the mechanism is unknown. Calcineurin was found to dephosphorylate BAD, a pro-apoptotic member of the Bcl-2 family, thus enhancing BAD heterodimerization with Bcl-x_L and promoting apoptosis. The Ca^{2+}-induced dephosphorylation of BAD correlated with its dissociation from 14-3-3 in the cytosol and translocation to mitochondria where Bcl-x_L resides. In hippocampal neurons, L-glutamate, an inducer of Ca^{2+} influx and calcineurin activation, triggered mitochondrial targeting of BAD and apoptosis, which were both suppressible by coexpression of a dominant-inhibitory mutant of calcineurin or pharmacological inhibitors of this phosphatase. Thus, a Ca^{2+}-inducible mechanism for apoptosis induction operates by regulating BAD phosphorylation and localization in cells.

Sustained increases in cytosolic-free Ca^{2+} lead to activation of the serine-threonine phosphatase (PPase) calcineurin (PPase-B) and subsequent apoptosis in susceptible cells (*1*). Overexpression of active calcineurin induces apoptosis through a mechanism that is suppressible by Bcl-2 (*2*). Bcl-2 family proteins regulate a distal step in an evolutionarily conserved pathway controlling apoptosis (*3*). Many Bcl-2 family proteins are anchored in the outer membranes of mitochondria, but oriented toward the cytosol. BAD is a pro-apoptotic member of this family that heterodimerizes with anti-apoptotic proteins such as Bcl-2 and Bcl-x_L, promoting cell death (*4*). Phosphorylation of BAD is induced by growth factors, impairing its binding to Bcl-x_L and abrogating its pro-apoptotic effects in cells (*5*). Several protein kinases can phosphorylate BAD, including Akt (*5*), which mediates cell survival signals within the phosphatidylinositol 3′ kinase pathway (*6*); protein kinase A (PKA) (*7*), a kinase previously implicated in cell survival (*8*); and Raf-1, which promotes cell survival when targeted to mitochondrial membranes through interactions with Bcl-2 (*9*).

We explored the possibility that phosphorylated BAD (phospho-BAD) might be a substrate of calcineurin involved in apoptosis. Transfection of 293T cells with a plasmid encoding a constitutively active form of calcineurin that lacks a negative regulatory domain (ΔCnA/B) (*2*) decreased ^{32}P incorporation into BAD (Fig. 1A). Coexpression of ΔCnA/B with either constitutively active Akt(E40K) (*6, 10*) or mitochondria-targeted active Raf-1 (M-Raf) (*9*) restored ^{32}P labeling of BAD. Experiments with a BAD mutant, BAD(S75E, S99E), in which two serines previously implicated in Akt-mediated phosphorylation (*5, 7, 9*) were replaced with an unphosphorylatable residue (glutamic acid), provided evidence that Akt and Raf-1 target different sites on BAD (Fig. 1B). However, regardless of whether active Akt or Raf-1 was used, coexpression of ΔCnA/B markedly reduced ^{32}P incorporation into BAD (Fig. 1B), suggesting that calcineurin can dephosphorylate multiple sites on this pro-apoptotic protein in cells. Consistent with a direct interaction, ΔCnA/B could be coimmunoprecipitated from lysates of 293T cells transfected with the BAD(S75E, S99E) protein, which mimics a phosphorylated form of BAD recognized as a substrate by this PPase (*11*).

Though a constitutively active form of calcineurin could induce dephosphorylation of BAD both in cells (Fig. 1, A and B) and in vitro (Fig. 1, C to E), we also examined whether endogenous calcineurin could associate with the endogenous BAD protein and control its phosphorylation state in untransfected cells. Calcineurin is the only known serine-threonine PPase whose activity is stimulated by Ca^{2+} (*12*). Changes in BAD phosphorylation were therefore examined in cells treated with Ca^{2+}-mobilizing agents, including the Ca^{2+} ionophores ionomycin and A23187 (*13*) and the endoplasmic reticulum Ca^{2+}–adenosine triphosphatase inhibitor thapsigargin (THG), which induces Ca^{2+} release from internal stores (*14*). HCT116 colon cancer and Du145 prostate cancer cells contain high endogenous phospho-BAD when grown with serum (*15*). Treatment of these cells with Ca^{2+}-mobilizing agents induced dephosphorylation of BAD, as determined by immunoblot analysis with antibodies specific to phospho-BAD, without altering the amount of BAD protein (Fig. 1F) (*13*). Akt kinase activity was unchanged under these same conditions (*13*), suggesting that the reduced amount of phospho-BAD was a result of active dephosphorylation of BAD rather than kinase suppression.

Coimmunoprecipitation experiments revealed that Ca^{2+}-mobilizing agents triggered dissociation of BAD from 14-3-3 (Fig. 1F). Moreover, endogenous calcineurin could be coimmunoprecipated with endogenous BAD before treatment with Ca^{2+}-mobilizing agents. In contrast, PPase-2A was not coimmunoprecipitated with BAD (Fig. 1G), indicating specificity of the calcineurin-BAD interaction. Interestingly, little or no calcineurin complexed with BAD after induction of dephosphorylation with Ca^{2+}-mobilizing agents (Fig. 1F). Thus, calcineurin appears to exist in a complex containing phospho-BAD before, but not after, Ca^{2+}-

[1]The Burnham Institute, 10901 North Torrey Pines Road, La Jolla, CA 92037, USA. [2]H. Lee Moffitt Cancer Center and Research Institute, Department of Pharmacology and Therapeutics, University of South Florida, Tampa, FL 33612, USA. [3]Department of Cell Biology, Harvard University, School of Medicine, Boston, MA 02115, USA. [4]Columbia University, Department of Pharmacology, 630 West 168 Street, New York, NY 10032, USA.

*These authors contributed equally to this work.
†To whom correspondence should be addressed: E-mail: jreed@burnham-institute.org